125 GeV Higgs decay with lepton flavor violation in the μνSSM *

Hai-Bin Zhang(张海斌)[1;1)] Tai-Fu Feng(冯太傅)[1,2;2)] Shu-Min Zhao(赵树民)[1], Yu-Li Yan(阎玉立)[1] Fei Sun(孙飞)[3]

[1] Department of Physics, Hebei University, Baoding 071002, China
[2] State Key Laboratory of Theoretical Physics (KLTP), Institute of Theoretical Physics, Chinese Academy of Sciences, Beijing 100190, China
[3] College of Science, China Three Gorges University, Yichang 443002, China

Abstract: Recently, the CMS and ATLAS collaborations have reported direct searches for the 125 GeV Higgs decay with lepton flavor violation, $\mathrm{h}\rightarrow\mu\tau$. In this work, we analyze the signal of the lepton flavour violating (LFV) Higgs decay $\mathrm{h}\rightarrow\mu\tau$ in the μ from ν Supersymmetric Standard Model (μνSSM) with slepton flavor mixing. Simultaneously, we consider the constraints from the LFV decay $\tau\rightarrow\mu\gamma$, the muon anomalous magnetic dipole moment and the lightest Higgs mass around 125 GeV.

Keywords: supersymmetry, Higgs decay, lepton flavor violation

PACS: 12.60.Jv, 14.80.Da, 11.30.Fs **DOI:** 10.1088/1674-1137/41/4/043106

1 Introduction

The discovery of the Higgs boson by the ATLAS and CMS Collaborations [1, 2] is a great success of the Large Hadron Collider (LHC). Combining the updated data of the ATLAS and CMS Collaborations, the measured mass of the Higgs boson now is [3]

$$m_{\mathrm{h}}=125.09\pm0.24\,\mathrm{GeV}. \quad (1)$$

The next step is focusing on searching for its properties. In the Standard Model (SM), which is renormalizable, lepton flavour violating (LFV) Higgs decays are forbidden [4]. But recently, a direct search for the 125 GeV Higgs decay with lepton flavor violation, $\mathrm{h}\rightarrow\mu\tau$, has been described by the CMS collaboration [5, 6]. The upper limit on the branching ratio of $\mathrm{h}\rightarrow\mu\tau$ at 95% confidence level (CL) is [6]

$$Br(\mathrm{h}\rightarrow\mu\tau)<1.20\times10^{-2}. \quad (2)$$

Here, interpreted as a signal, $\mu\tau$ means the final state consisting of $\bar{\mu}\tau$ and $\mu\bar{\tau}$.

The ATLAS Collaboration gives the constraint on the branching ratio of $\mathrm{h}\rightarrow\mu\tau$ at 95% CL to be [7, 8]

$$Br(\mathrm{h}\rightarrow\mu\tau)<1.43\times10^{-2}. \quad (3)$$

The ATLAS and CMS experiments do not currently show a significant deviation from the SM. Therefore, the experiments still need to make more precise measurements in the future.

LFV Higgs decays can occur naturally in models beyond the SM, such as supersymmetric models [9–17], composite Higgs boson models [18, 19], Randall-Sundrum models [20–22], and many others [23–40]. Due to the running of the LHC, LFV Higgs decays have recently been discussed within various theoretical frameworks [41–105]. In this paper, we will study the LFV Higgs decay $\mathrm{h}\rightarrow\mu\tau$ in the "μ from ν Supersymmetric Standard Model" (μνSSM) [106–108]. As an extension of the Minimal Supersymmetric Standard Model (MSSM) [109–113], the μνSSM solves the μ problem [114] of the MSSM, through the R-parity breaking couplings $\lambda_i\hat{\nu}^c_i\hat{H}^a_d\hat{H}^b_u$ in the superpotential. The μ term is generated spontaneously via the nonzero vacuum expectative values (VEVs) of right-handed sneutrinos, $\mu=\lambda_i\langle\tilde{\nu}^c_i\rangle$, when the electroweak symmetry is broken (EWSB). In addition, nonzero VEVs of sneutrinos in the μνSSM can generate three tiny massive Majorana

Received 05 September 2016, Revised 21 November 2016

∗ Supported by Major Project of NNSFC (11535002) and NNSFC (11275036, 11647120), the Open Project Program of State Key Laboratory of Theoretical Physics, Institute of Theoretical Physics, Chinese Academy of Sciences, China (Y5KF131CJ1), the Natural Science Foundation of Hebei province (A2013201277, A2016201010, A2016201069), Hebei Key Lab of Optic-Electronic Information and Materials, and Midwest Universities Comprehensive Strength Promotion Project

1) E-mail: hbzhang@hbu.edu.cn

2) E-mail: fengtf@hbu.edu.cn

neutrinos at tree level through the seesaw machanism [106–108, 115-119].

Within the μνSSM, we have studied some LFV processes, $l_j^- \to l_i^- \gamma$, $l_j^- \to l_i^- l_i^- l_i^+$, muon conversion to electrons in nuclei and $Z \to l_i^{\pm} l_j^{\mp}$ in our previous work [120–122]. The numerical results show that the LFV rates for $l_j - l_i$ transitions in the μνSSM depend on the slepton flavor mixing, and the present experimental limits for the branching ratio of $l_j^- \to l_i^- \gamma$ constrain the slepton mixing parameters most strictly [122]. In this work, considering the constraint of $\tau \to \mu\gamma$, we continue to analyze the LFV Higgs decay $h \to \mu\tau$ in the μνSSM with slepton flavor mixing.

The paper is organized as follows. In Section 2, we briefly present the μνSSM, including its superpotential and the general soft SUSY-breaking terms. Section 3 contains the analytical expressions of the 125 GeV Higgs decay with lepton flavor violation in the μνSSM. The numerical analysis and the summary are given in Section 4 and Section 5, respectively. Some formulae are collected in Appendix and Appendix .

2 The μνSSM

In addition to the superfields of the MSSM, the μνSSM introduces right-handed neutrino superfields $\hat{\nu}_i^c$ $(i=1,2,3)$. Besides the MSSM Yukawa couplings for quarks and charged leptons, the superpotential of the μνSSM contains Yukawa couplings for neutrinos, two additional types of terms involving the Higgs doublet superfields $\hat{H}_u$ and $\hat{H}_d$, and the right-handed neutrino superfields $\hat{\nu}_i^c$, [106]

$$W = \epsilon_{ab}\left(Y_{u_{ij}}\hat{H}_u^b\hat{Q}_i^a\hat{u}_j^c + Y_{d_{ij}}\hat{H}_d^a\hat{Q}_i^b\hat{d}_j^c + Y_{e_{ij}}\hat{H}_d^a\hat{L}_i^b\hat{e}_j^c\right) + \epsilon_{ab}Y_{\nu_{ij}}\hat{H}_u^b\hat{L}_i^a\hat{\nu}_j^c - \epsilon_{ab}\lambda_i\hat{\nu}_i^c\hat{H}_d^a\hat{H}_u^b + \frac{1}{3}\kappa_{ijk}\hat{\nu}_i^c\hat{\nu}_j^c\hat{\nu}_k^c, \quad (4)$$

where $\hat{H}_u^T = \left(\hat{H}_u^+, \hat{H}_u^0\right)$, $\hat{H}_d^T = \left(\hat{H}_d^0, \hat{H}_d^-\right)$, $\hat{Q}_i^T = \left(\hat{u}_i, \hat{d}_i\right)$, $\hat{L}_i^T = \left(\hat{\nu}_i, \hat{e}_i\right)$ are $SU(2)$ doublet superfields, and $\hat{u}_i^c$, $\hat{d}_i^c$, and $\hat{e}_i^c$ denote the singlet up-type quark, down-type quark and charged lepton superfields, respectively. Here, Y, λ, and κ are dimensionless matrices, a vector, and a totally symmetric tensor. $i,j,k=1,2,3$ are the generation indices, $a,b=1,2$ are the SU(2) indices with antisymmetric tensor $\epsilon_{12}=1$. In the superpotential, the last two terms explicitly violate lepton number and R-parity. Note that the summation convention is implied on repeated indices in this paper.

Once EWSB occurs, the neutral scalars develop in general the VEVs:

$$\langle H_d^0\rangle = \upsilon_d, \quad \langle H_u^0\rangle = \upsilon_u, \quad \langle\tilde{\nu}_i\rangle = \upsilon_{\nu_i}, \quad \langle\tilde{\nu}_i^c\rangle = \upsilon_{\nu_i^c}. \quad (5)$$

Then, the terms $\epsilon_{ab}Y_{\nu_{ij}}\hat{H}_u^b\hat{L}_i^a\hat{\nu}_j^c$ and $\epsilon_{ab}\lambda_i\hat{\nu}_i^c\hat{H}_d^a\hat{H}_u^b$ in the superpotential can generate the effective bilinear terms $\epsilon_{ab}\varepsilon_i\hat{H}_u^b\hat{L}_i^a$ and $\epsilon_{ab}\mu\hat{H}_d^a\hat{H}_u^b$, with $\varepsilon_i = Y_{\nu_{ij}}\langle\tilde{\nu}_j^c\rangle$ and $\mu = \lambda_i\langle\tilde{\nu}_i^c\rangle$. One can define the neutral scalars as

$$H_d^0 = \frac{h_d + \mathrm{i}P_d}{\sqrt{2}} + \upsilon_d, \quad \tilde{\nu}_i = \frac{(\tilde{\nu}_i)^{\Re} + \mathrm{i}(\tilde{\nu}_i)^{\Im}}{\sqrt{2}} + \upsilon_{\nu_i},$$
$$H_u^0 = \frac{h_u + \mathrm{i}P_u}{\sqrt{2}} + \upsilon_u, \quad \tilde{\nu}_i^c = \frac{(\tilde{\nu}_i^c)^{\Re} + \mathrm{i}(\tilde{\nu}_i^c)^{\Im}}{\sqrt{2}} + \upsilon_{\nu_i^c}. \quad (6)$$

In the framework of supergravity-mediated supersymmetry breaking, the general soft SUSY-breaking terms of the μνSSM are given by

$$\begin{aligned}
-\mathcal{L}_{\rm soft} &= m_{\tilde{Q}_{ij}}^2\tilde{Q}_i^{a*}\tilde{Q}_j^a + m_{\tilde{u}_{ij}^c}^2\tilde{u}_i^{c*}\tilde{u}_j^c + m_{\tilde{d}_{ij}^c}^2\tilde{d}_i^{c*}\tilde{d}_j^c + m_{\tilde{L}_{ij}}^2\tilde{L}_i^{a*}\tilde{L}_j^a \\
&+ m_{\tilde{e}_{ij}^c}^2\tilde{e}_i^{c*}\tilde{e}_j^c + m_{H_d}^2 H_d^{a*}H_d^a + m_{H_u}^2 H_u^{a*}H_u^a + m_{\tilde{\nu}_{ij}^c}^2\tilde{\nu}_i^{c*}\tilde{\nu}_j^c \\
&+ \epsilon_{ab}\Big[(A_uY_u)_{ij}H_u^b\tilde{Q}_i^a\tilde{u}_j^c + (A_dY_d)_{ij}H_d^a\tilde{Q}_i^b\tilde{d}_j^c \\
&+ (A_eY_e)_{ij}H_d^a\tilde{L}_i^b\tilde{e}_j^c + \mathrm{H.c.}\Big] + \Big[\epsilon_{ab}(A_\nu Y_\nu)_{ij}H_u^b\tilde{L}_i^a\tilde{\nu}_j^c \\
&- \epsilon_{ab}(A_\lambda\lambda)_i\tilde{\nu}_i^c H_d^a H_u^b + \frac{1}{3}(A_\kappa\kappa)_{ijk}\tilde{\nu}_i^c\tilde{\nu}_j^c\tilde{\nu}_k^c + \mathrm{H.c.}\Big] \\
&- \frac{1}{2}\Big(M_3\tilde{\lambda}_3\tilde{\lambda}_3 + M_2\tilde{\lambda}_2\tilde{\lambda}_2 + M_1\tilde{\lambda}_1\tilde{\lambda}_1 + \mathrm{H.c.}\Big). \quad (7)
\end{aligned}$$

Here, the first two lines contain mass squared terms of squarks, sleptons, Higgses and sneutrinos. The next three lines include the trilinear scalar couplings. In the last line, M_3, M_2, and M_1 represent the Majorana masses corresponding to $SU(3)$, $SU(2)$, and $U(1)$ gauginos $\hat{\lambda}_3$, $\hat{\lambda}_2$, and $\hat{\lambda}_1$, respectively. In addition, the tree-level scalar potential receives the usual D- and F-term contributions [107].

In the μνSSM, the quadratic potential includes

$$V_{\rm quadratic} = \frac{1}{2}S'^T M_S^2 S' + \frac{1}{2}P'^T M_P^2 P' + S'^{-T}M_{S^\pm}^2 S'^+ + (\frac{1}{2}\chi'^{0T}M_n\chi'^0 + \Psi^{-T}M_c\Psi^+ + \mathrm{H.c.}) + \cdots, \quad (8)$$

where in the unrotated basis $S'^T = (h_d, h_u, (\tilde{\nu}_i)^{\Re}, (\tilde{\nu}_i^c)^{\Re})$, $P'^T = (P_d, P_u, (\tilde{\nu}_i)^{\Im}, (\tilde{\nu}_i^c)^{\Im})$, $S'^{\pm T} = (H_d^\pm, H_u^\pm, \tilde{e}_{L_i}^\pm, \tilde{e}_{R_i}^\pm)$, $\Psi^{-T} = \left(-i\tilde{\lambda}^-, \tilde{H}_d^-, e_{L_i}^-\right)$, $\Psi^{+T} = \left(-i\tilde{\lambda}^+, \tilde{H}_u^+, e_{R_i}^+\right)$ and $\chi'^{0T} = \left(\tilde{B}^0, \tilde{W}^0, \tilde{H}_d, \tilde{H}_u, \nu_{R_i}, \nu_{L_i}\right)$. The concrete expressions for the independent coefficients of mass matrices M_S^2, M_P^2, $M_{S^\pm}^2$, M_n and M_c can be found in Ref. [121]. Using 8×8 unitary matrices R_S, R_P and $R_{S^\pm}$, the unrotated basises S', P' and $S^{\pm\prime}$ can be respectively rotated to the mass eigenvectors S, P and $S^\pm$:

$$S' = R_S S, \quad P' = R_P P, \quad S^{\pm\prime} = R_{S^\pm}S^\pm. \quad (9)$$

Through the unitary matrices Z_n, Z_- and Z_+, neutral and charged fermions can also be rotated to the mass eigenvectors χ^0 and χ, respectively.

3 125 GeV Higgs decay with lepton flavor violation

The corresponding effective amplitude for 125 GeV Higgs decay with lepton flavor violation $\mathrm{h}\to\bar{l}_i l_j$ can be written as

$$\mathcal{M}=\bar{l}_i(F_L^{ij}P_L+F_R^{ij}P_R)l_j, \tag{10}$$

with

$$F_{L,R}^{ij}=F_{L,R}^{(V)ij}+F_{L,R}^{(S)ij}, \tag{11}$$

where $F_{L,R}^{(V)ij}$ denotes the contributions from the vertex diagrams in Fig. 1, and $F_{L,R}^{(S)ij}$ stands for the contributions from the self-energy diagrams in Fig. 2, respectively.

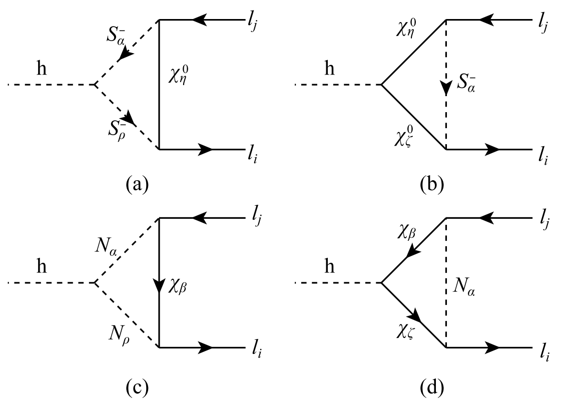

Fig. 1. Vertex diagrams for $\mathrm{h}\to\bar{l}_i l_j$. (a,b) represent the contributions from charged scalar $S^-_{\alpha,\rho}$ and neutral fermion $\chi^0_{\eta,\varsigma}$ loops, while (c,d) represent the contributions from neutral scalar $N_{\alpha,\rho}$ $(N=S,P)$ and charged fermion $\chi_{\beta,\zeta}$ loops.

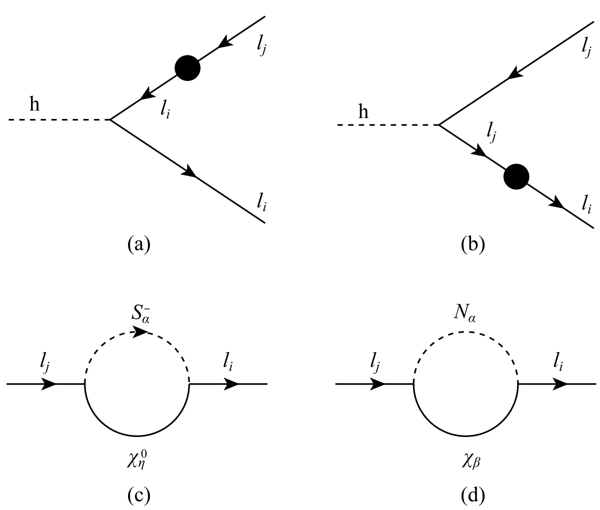

Fig. 2. Self-energy diagrams contributing to $\mathrm{h}\to\bar{l}_i l_j$ in the μνSSM. The blob in (a,b) indicates the self-energy contributions from (c,d).

The one-loop vertex diagrams for $\mathrm{h}\to\bar{l}_i l_j$ in the μνSSM are depicted by Fig. 1. Then, we can have

$$F_{L,R}^{(V)ij}=F_{L,R}^{(a)ij}+F_{L,R}^{(b)ij}+F_{L,R}^{(c)ij}+F_{L,R}^{(d)ij}, \tag{12}$$

where $F_{L,R}^{(a,b)ij}$ denotes the contributions from charged scalar $S^-_{\alpha,\rho}$ and neutral fermion $\chi^0_{\eta,\varsigma}$ loops, and $F_{L,R}^{(c,d)ij}$ stands for the contributions from the neutral scalar $N_{\alpha,\rho}$ $(N=S,P)$ and charged fermion $\chi_{\beta,\zeta}$ loops, respectively. After integrating the heavy freedoms out, we formulate the neutral fermion loop contributions $F_{L,R}^{(a,b)ij}$ as follows:

$$\begin{aligned}
F_L^{(a)ij}&=\frac{m_{\chi^0_\eta}C^{S^\pm}_{1\alpha\rho}}{m_{\mathrm{W}}^2}C_L^{S^-_\rho\chi^0_\eta\bar{l}_i}C_L^{S^{-}_\alpha{}^* l_j\bar{\chi}^0_\eta}G_1(x_{\chi^0_\eta},x_{S^-_\alpha},x_{S^-_\rho}),\\
F_L^{(b)ij}&=\frac{m_{\chi^0_\varsigma}m_{\chi^0_\eta}}{m_{\mathrm{W}}^2}C_L^{S^-_\alpha\chi^0_\varsigma\bar{l}_i}C_L^{h\chi^0_\eta\bar{\chi}^0_\varsigma}C_L^{S^{-}_\alpha{}^* l_j\bar{\chi}^0_\eta}G_1(x_{S^-_\alpha},x_{\chi^0_\varsigma},x_{\chi^0_\eta})\\
&\quad+C_L^{S^-_\alpha\chi^0_\varsigma\bar{l}_i}C_R^{h\chi^0_\eta\bar{\chi}^0_\varsigma}C_L^{S^{-}_\alpha{}^* l_j\bar{\chi}^0_\eta}G_2(x_{S^-_\alpha},x_{\chi^0_\varsigma},x_{\chi^0_\eta}),\\
F_R^{(a,b)ij}&=F_L^{(a,b)ij}\Big|_{L\leftrightarrow R}.
\end{aligned} \tag{13}$$

Here, the concrete expressions for couplings C (and below) can be found in Appendix A and Ref. [123], $x=m^2/m_{\mathrm{W}}^2$, m is the mass for the corresponding particle, and the loop functions G_i are given as

$$\begin{aligned}
G_1(x_1,x_2,x_3)&=\frac{1}{16\pi^2}\Big[\frac{x_1\ln x_1}{(x_2-x_1)(x_1-x_3)}\\
&\quad+\frac{x_2\ln x_2}{(x_1-x_2)(x_2-x_3)}+\frac{x_3\ln x_3}{(x_1-x_3)(x_3-x_2)}\Big],
\end{aligned} \tag{14}$$

$$\begin{aligned}
G_2(x_1,x_2,x_3)&=\frac{1}{16\pi^2}\Big[\frac{x_1^2\ln x_1}{(x_2-x_1)(x_1-x_3)}\\
&\quad+\frac{x_2^2\ln x_2}{(x_1-x_2)(x_2-x_3)}+\frac{x_3^2\ln x_3}{(x_1-x_3)(x_3-x_2)}\Big].
\end{aligned} \tag{15}$$

In a similar way, the charged fermion loop contributions $F_{L,R}^{(c,d)ij}$ are

$$\begin{aligned}
F_L^{(c)ij}&=\sum_{N=S,P}\frac{m_{\chi_\beta}C^N_{1\alpha\rho}}{m_{\mathrm{W}}^2}C_L^{N_\rho\chi_\beta\bar{l}_i}C_L^{N_\alpha l_j\bar{\chi}_\beta}G_1(x_{\chi_\beta},x_{N_\alpha},x_{N_\rho}),\\
F_L^{(d)ij}&=\sum_{N=S,P}\Big[C_L^{N_\alpha\chi_\zeta\bar{l}_i}C_R^{\mathrm{h}\chi_\beta\bar{\chi}_\zeta}C_L^{N_\alpha l_j\bar{\chi}_\beta}G_2(x_{N_\alpha},x_{\chi_\zeta},x_{\chi_\beta})\\
&\quad+\frac{m_{\chi_\zeta}m_{\chi_\beta}}{m_{\mathrm{W}}^2}C_L^{N_\alpha\chi_\zeta\bar{l}_i}C_L^{\mathrm{h}\chi_\beta\bar{\chi}_\zeta}C_L^{N_\alpha l_j\bar{\chi}_\beta}G_1(x_{N_\alpha},x_{\chi_\zeta},x_{\chi_\beta})\Big],\\
F_R^{(c,d)ij}&=F_L^{(c,d)ij}\Big|_{L\leftrightarrow R}.
\end{aligned} \tag{16}$$

In Fig. 2, we show the self-energy diagrams contributing to $\mathrm{h}\to\bar{l}_i l_j$ in the μνSSM. The contributions from the self-energy diagrams $F_{L,R}^{(S)ij}$ can be given as

$$F_{L,R}^{(S)ij}=F_{L,R}^{(Sa)ij}+F_{L,R}^{(Sb)ij}, \tag{17}$$

with

$$F_L^{(Sa)ij}=\frac{C_L^{\mathrm{h}l_i\bar{l}_i}}{m_{l_j}^2-m_{l_i}^2}\Big\{m_{l_j}^2\Sigma_R(m_{l_j}^2)+m_{l_j}^2\Sigma_{Rs}(m_{l_j}^2)$$
$$+m_{l_i}[m_{l_j}\Sigma_L(m_{l_j}^2)+m_{l_j}\Sigma_{Ls}(m_{l_j}^2)]\Big\},$$
$$F_L^{(Sb)ij}=\frac{C_L^{\mathrm{h}l_j\bar{l}_j}}{m_{l_i}^2-m_{l_j}^2}\Big\{m_{l_i}^2\Sigma_L(m_{l_i}^2)+m_{l_i}m_{l_j}\Sigma_{Rs}(m_{l_i}^2)$$
$$+m_{l_j}[m_{l_i}\Sigma_R(m_{l_i}^2)+m_{l_j}\Sigma_{Ls}(m_{l_i}^2)]\Big\},$$
$$F_R^{(Sa,Sb)ij}=F_L^{(Sa,Sb)ij}\Big|_{L\leftrightarrow R}. \tag{18}$$

The Σ of the self-energy diagrams in Fig. 2(c,d) can be obtained below

$$\Sigma_L(p^2)=-\frac{1}{16\pi^2}\Big\{B_1(p^2,m_{\chi_\eta^0}^2,m_{S_\alpha^-}^2)C_L^{S_\alpha^-\chi_\eta^0\bar{l}_i}C_R^{S_\alpha^{-*}l_j\bar{\chi}_\eta^0}$$
$$+\sum_{N=S,P}B_1(p^2,m_{\chi_\beta}^2,m_{N_\alpha}^2)$$
$$\cdot C_L^{N_\alpha\chi_\beta\bar{l}_i}C_R^{N_\alpha l_j\bar{\chi}_\beta}\Big\},$$
$$m_{l_j}\Sigma_{Ls}(p^2)=\frac{1}{16\pi^2}\Big\{m_{\chi_\eta^0}B_0(p^2,m_{\chi_\eta^0}^2,m_{S_\alpha^-}^2)$$
$$C_L^{S_\alpha^-\chi_\eta^0\bar{l}_i}C_L^{S_\alpha^{-*}l_j\bar{\chi}_\eta^0}$$
$$+\sum_{N=S,P}m_{\chi_\beta}B_0(p^2,m_{\chi_\beta}^2,m_{N_\alpha}^2)$$
$$C_L^{N_\alpha\chi_\beta\bar{l}_i}C_L^{N_\alpha l_j\bar{\chi}_\beta}\Big\},$$
$$\Sigma_R(p^2)=\Sigma_L(p^2)|_{L\leftrightarrow R},$$
$$m_{l_j}\Sigma_{Rs}(p^2)=m_{l_j}\Sigma_{Ls}(p^2)\big|_{L\leftrightarrow R}. \tag{19}$$

Here, $B_{0,1}(p^2,m_0^2,m_1^2)$ are two-point functions [124–130].

Then, we can obtain the decay width of $\mathrm{h}\to\bar{l}_il_j$ [9, 14]

$$\Gamma(\mathrm{h}\to\bar{l}_il_j)\approx\frac{m_\mathrm{h}}{16\pi}\Big(\big|F_L^{ij}\big|^2+\big|F_R^{ij}\big|^2\Big). \tag{20}$$

If interpreted as a signal, the decay width of $\mathrm{h}\to l_il_j$ is

$$\Gamma(\mathrm{h}\to l_il_j)=\Gamma(\mathrm{h}\to\bar{l}_il_j)+\Gamma(\mathrm{h}\to\bar{l}_jl_i), \tag{21}$$

and the branching ratio of $\mathrm{h}\to l_il_j$ is

$$Br(\mathrm{h}\to l_il_j)=\Gamma(\mathrm{h}\to l_il_j)/\Gamma_h, \tag{22}$$

where $\Gamma_\mathrm{h}\approx4.1\times10^{-3}$ GeV [131] denotes the total decay width of the 125 GeV Higgs boson.

4 Numerical analysis

In order to obtain transparent numerical results in the μνSSM, we take the minimal flavor violation (MFV) assumptions for some parameters, which assume

$$\kappa_{ijk}=\kappa\delta_{ij}\delta_{jk},\quad(A_\kappa\kappa)_{ijk}=A_\kappa\kappa\delta_{ij}\delta_{jk},\quad\lambda_i=\lambda,$$
$$(A_\lambda\lambda)_i=A_\lambda\lambda,\quad Y_{e_{ij}}=Y_{e_i}\delta_{ij},\quad Y_{\nu_{ij}}=Y_{\nu_i}\delta_{ij},$$
$$\upsilon_{\nu_i^c}=\upsilon_{\nu^c},\quad(A_\nu Y_\nu)_{ij}=a_{\nu_i}\delta_{ij},\quad m_{\tilde{\nu}_{ij}^c}^2=m_{\tilde{\nu}_i^c}^2\delta_{ij},$$
$$m_{\tilde{Q}_{ij}}^2=m_{\tilde{Q}_i}^2\delta_{ij},\quad m_{\tilde{u}_{ij}^c}^2=m_{\tilde{u}_i^c}^2\delta_{ij},\quad m_{\tilde{d}_{ij}^c}^2=m_{\tilde{d}_i^c}^2\delta_{ij}, \tag{23}$$

where $i,\ j,\ k=1,\ 2,\ 3$. $m_{\tilde{\nu}_i^c}^2$ can be constrained by the minimization conditions of the neutral scalar potential seen in Ref. [121]. To agree with experimental observations on quark mixing, one can have

$$Y_{u_{ij}}=Y_{u_i}V_{L_{ij}}^u,\quad(A_uY_u)_{ij}=A_{u_i}Y_{u_{ij}},$$
$$Y_{d_{ij}}=Y_{d_i}V_{L_{ij}}^d,\quad(A_dY_d)_{ij}=A_{d_i}Y_{d_{ij}}, \tag{24}$$

and $V=V_L^uV_L^{d\dagger}$ denotes the CKM matrix.

For the trilinear coupling matrix (A_eY_e) and soft breaking slepton mass matrices $m_{\tilde{L},\tilde{e}^c}^2$, we will take into account the off-diagonal terms for the matrices, which are named the slepton flavor mixings and are defined by [132–137]

$$m_{\tilde{L}}^2=\begin{pmatrix}1&\delta_{12}^{LL}&\delta_{13}^{LL}\\\delta_{12}^{LL}&1&\delta_{23}^{LL}\\\delta_{13}^{LL}&\delta_{23}^{LL}&1\end{pmatrix}m_L^2, \tag{25}$$

$$m_{\tilde{e}^c}^2=\begin{pmatrix}1&\delta_{12}^{RR}&\delta_{13}^{RR}\\\delta_{12}^{RR}&1&\delta_{23}^{RR}\\\delta_{13}^{RR}&\delta_{23}^{RR}&1\end{pmatrix}m_E^2, \tag{26}$$

$$(A_eY_e)=\begin{pmatrix}m_{l_1}A_e&\delta_{12}^{LR}m_Lm_E&\delta_{13}^{LR}m_Lm_E\\\delta_{12}^{LR}m_Lm_E&m_{l_2}A_e&\delta_{23}^{LR}m_Lm_E\\\delta_{13}^{LR}m_Lm_E&\delta_{23}^{LR}m_Lm_E&m_{l_3}A_e\end{pmatrix}\frac{1}{\upsilon_d}. \tag{27}$$

The following numerical results will show that the branching ratio of $\mathrm{h}\to\mu\tau$ depends on the slepton mixing parameters δ_{23}^{XX} $(X=L,R)$.

At first, the constraints from some experiments should be considered. Through our previous work [119], we have discussed in detail how the neutrino oscillation data constrain neutrino Yukawa couplings $Y_{\nu_i}\sim\mathcal{O}(10^{-7})$ and left-handed sneutrino VEVs $\upsilon_{\nu_i}\sim\mathcal{O}(10^{-4}\mathrm{GeV})$ via the seesaw mechanism. Here, due to the neutrino sector only weakly affecting $\mathrm{h}\to\mu\tau$, we can take no account of the constraints from neutrino experiment data.

The neutral Higgs with mass around 125 GeV reported by ATLAS and CMS contributes a strict constraint on the relevant parameters of the μνSSM. For a large mass of the pseudoscalar M_A and moderate $\tan\beta$, the SM-like Higgs mass of the μνSSM is approximately written as [107, 138]

$$m_\mathrm{h}^2\approx qm_\mathrm{Z}^2\cos^22\beta+\frac{6\lambda^2s_\mathrm{W}^2c_\mathrm{W}^2}{e^2}m_\mathrm{Z}^2\sin^22\beta+\Delta m_\mathrm{h}^2. \tag{28}$$

Compared with the MSSM, the μνSSM gets an additional term, $\frac{6\lambda^2 s_W^2 c_W^2}{e^2} m_Z^2 \sin^2 2\beta$. Thus, the SM-like Higgs in the μνSSM can easily account for the mass around 125 GeV, especially for small $\tan\beta$. Including two-loop leading-log effects, the main radiative corrections Δm_h^2 can be given as [139–141]

$$\Delta m_h^2 = \frac{3m_t^4}{4\pi^2 \upsilon^2}\Big[\Big(t+\frac{1}{2}\tilde{X}_t\Big) + \frac{1}{16\pi^2}\Big(\frac{3m_t^2}{2\upsilon^2}-32\pi\alpha_3\Big)(t^2+\tilde{X}_t t)\Big],$$

$$t=\log\frac{M_S^2}{m_t^2}, \qquad \tilde{X}_t=\frac{2\tilde{A}_t^2}{M_S^2}\Big(1-\frac{\tilde{A}_t^2}{12M_S^2}\Big), \tag{29}$$

where $\upsilon = 174$ GeV, α_3 is the strong coupling constant, $M_S = \sqrt{m_{\tilde{t}_1} m_{\tilde{t}_2}}$ with $m_{\tilde{t}_{1,2}}$ denoting the stop masses, $\tilde{A}_t = A_t - \mu\cot\beta$ with $A_t = A_{u_3}$ being the trilinear Higgs-stop coupling and $\mu = 3\lambda\upsilon_{\nu^c}$ denoting the Higgsino mass parameter.

We also impose a constraint on the SUSY contribution to the muon magnetic dipole moment a_μ in the μνSSM, which is given in Appendix for convenience. The difference between experiment and the SM prediction on a_μ is [142–144]

$$\Delta a_\mu = a_\mu^{\rm exp} - a_\mu^{\rm SM} = (24.8 \pm 7.9)\times 10^{-10}, \tag{30}$$

with all errors combining in quadrature. Therefore, the SUSY contribution to a_μ in the μνSSM should be constrained as $1.1\times10^{-10} \leqslant \Delta a_\mu \leqslant 48.5\times 10^{-10}$, where a 3σ experimental error is considered.

Through analysis of the parameter space of the μνSSM in Ref. [107], we can take reasonable parameter values to be $\lambda = 0.1$, $\kappa = 0.4$, $A_\lambda = 500$ GeV, $A_\kappa = -300$ GeV and $A_e = 1$ TeV for simplicity. For the gauginos' Majorana masses, we will choose the approximate GUT relation $M_1 = \frac{\alpha_1^2}{\alpha_2^2} M_2 \approx 0.5 M_2$ and $M_3 = \frac{\alpha_3^2}{\alpha_2^2} M_2 \approx 2.7 M_2$. The gluino mass, $m_{\tilde{g}} \approx M_3$, is greater than about 1.2 TeV from the ATLAS and CMS experimental data [145–148]. For simplicity, we could adopt $m_{\tilde{Q}_3} = m_{\tilde{u}_3^c} = m_{\tilde{d}_3^c} = 1.5$ TeV. As key parameters, A_t and $\tan\beta \equiv \upsilon_u/\upsilon_d$ affect the SM-like Higgs mass. Here, we keep the SM-like Higgs mass $m_h = 125$ GeV as input, and then the value of parameter A_t can be given automatically in the numerical calculation. Then, the free parameters that affect our next analysis are $\tan\beta$, $\mu \equiv 3\lambda\upsilon_{\nu^c}$, M_2, m_L, m_E and slepton mixing parameters δ_{23}^{XX} $(X=L,R)$.

It is well known that the lepton flavour violating processes are flavor dependent. The LFV rates for $\mu-\tau$ transitions depend on the slepton mixing parameters δ_{23}^{XX} $(X = L,R)$, which can be confirmed by Fig. 3. The slepton mixing parameters δ_{12}^{XX} and δ_{13}^{XX} $(X=L,R)$ hardly affect the LFV rates for $\mu-\tau$ transitions, which play a leading role in the LFV rates for $e-\mu$ and $e-\tau$ transitions. So, we take $\delta_{12}^{XX}=0$ and $\delta_{13}^{XX}=0$ $(X=L,R)$ here. To produce Fig. 3, we scan the parameter space shown in Table 1. Here the steps are large, because the running of the program is not very fast. However the scanned parameter space is broad enough to contain the possibility of more.

In the scan, we keep the chargino masses $m_{\chi_\beta} > 200$ GeV $(\beta=1,2)$, the neutral fermion masses $m_{\chi_\eta^0} > 200$ GeV $(\eta=1,\cdots,7)$, and the scalar masses $m_{S_\alpha,P_\alpha,S_\alpha^\pm} >$ 500 GeV $(\eta = 2,\cdots,8)$, to avoid the range ruled out by the experiments [142]. The results are also constrained by the muon anomalous magnetic dipole moment $1.1\times10^{-10} \leqslant \Delta a_\mu \leqslant 48.5\times10^{-10}$, where a 3σ experimental error is considered. In Ref. [123], we have investigated the signals of the Higgs boson decay channels $h\to\gamma\gamma$, $h\to VV^*$ $(V=Z,W)$, and $h\to f\bar{f}$ $(f=b,\tau)$ in the μνSSM. When the lightest stop mass $m_{\tilde{t}_1} \gtrsim 700$ GeV and the lightest stau mass $m_{\tilde{\tau}_1} \gtrsim 300$ GeV, the signal strengths of these Higgs boson decay channels are in agreement with the SM. Therefore, the scanning results in this paper coincide with the experimental data of these Higgs boson decay channels.

Note that, when the calculation program is scanning one of the slepton mixing parameters δ_{23}^{XX} $(X=L,R)$, the other two slepton mixing parameters δ_{23}^{XX} $(X=L,R)$ are set to zero. So, we can see the contribution of every slepton mixing parameter alone. Then in Fig. 3, we plot $Br(h\to\mu\tau)$ varying with slepton mixing parameters δ_{23}^{LR} (a), δ_{23}^{LL} (c), and δ_{23}^{RR} (e) respectively, where the dashed line stands for the upper limit on $Br(h\to\mu\tau)$ at 95% CL shown in Eq. (2). We also plot $Br(\tau\to\mu\gamma)$ versus slepton mixing parameters δ_{23}^{LR} (b), δ_{23}^{LL} (d), and δ_{23}^{RR} (f) respectively, where the dashed line denotes the present limit of $Br(\tau\to\mu\gamma)$ [149]:

$$Br(\tau\to\mu\gamma) < 4.4\times10^{-8}. \tag{31}$$

Here, the red triangles are ruled out by the present limit of $Br(\tau\to\mu\gamma)$, and the black circles are consistent with the present limit of $Br(\tau\to\mu\gamma)$.

In Fig. 3, when slepton mixing parameters $\delta_{23}^{XX} = 0$ $(X=L,R)$, $Br(h\to\mu\tau)$ can reach $\mathcal{O}(10^{-23})$ and $Br(\tau\to\mu\gamma)$ can attain $\mathcal{O}(10^{-27})$, because the contributions can come from the mixing of the particles, which can easily be seen in Eq. (8). These results are too small to detect. However, if the nonzero slepton mixing parameters δ_{23}^{XX} $(X=L,R)$ are considered, $Br(h\to\mu\tau)$ and $Br(\tau\to\mu\gamma)$ grow quickly. With increasing δ_{23}^{XX} $(X=L,R)$, $Br(\tau\to\mu\gamma)$ can easily go beyond the present experimental limit of $Br(\tau\to\mu\gamma)$, shown in the plot as the red triangles. Although $Br(h\to\mu\tau)$ cannot reach

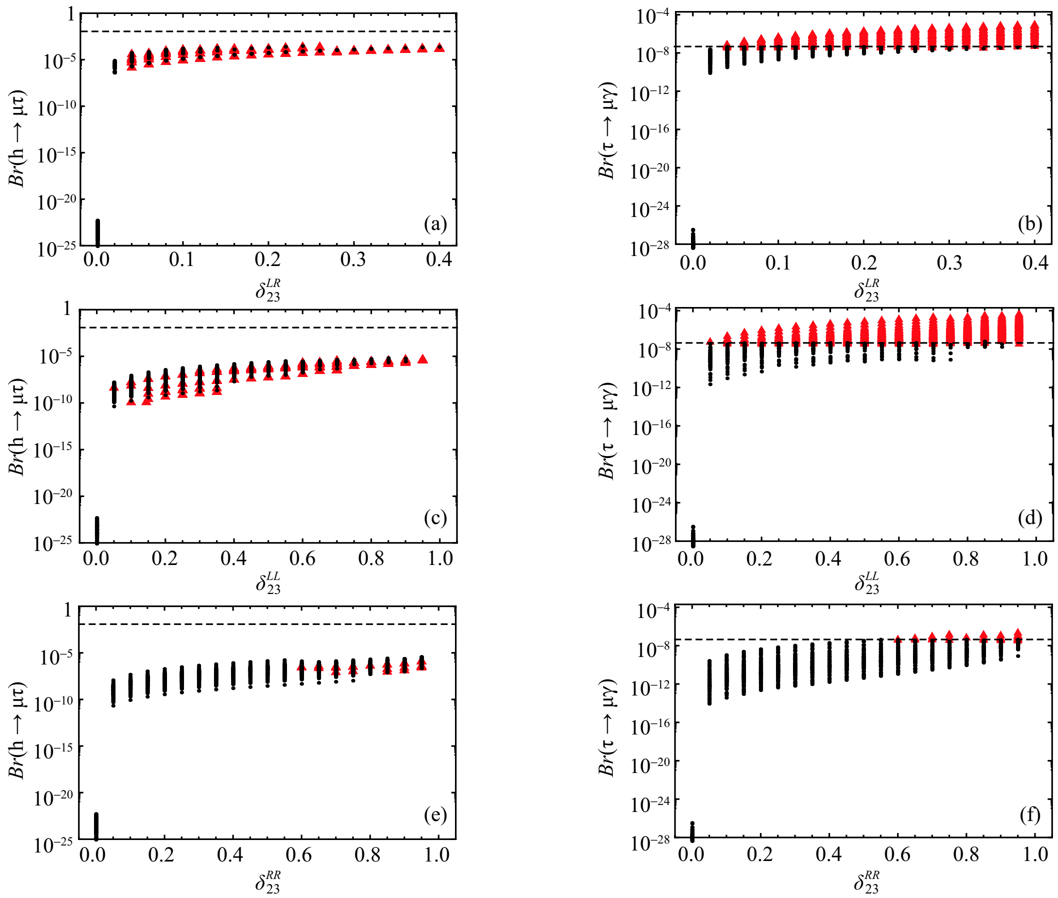

Fig. 3. (color online) $Br(\mathrm{h}\to\mu\tau)$ versus slepton mixing parameters δ_{23}^{LR} (a), δ_{23}^{LL} (c), and δ_{23}^{RR} (e), where the dashed line stands for the upper limit on $Br(\mathrm{h}\to\mu\tau)$ at 95% CL showed in Eq. (2). $Br(\tau\to\mu\gamma)$ versus slepton mixing parameters δ_{23}^{LR} (b), δ_{23}^{LL} (d), and δ_{23}^{RR} (f), where the dashed line denotes the present limit of $Br(\tau\to\mu\gamma)$ seen in Eq. (31). Here, the red triangles are ruled out by the present limit of $Br(\tau\to\mu\gamma)$, and the black circles are consistent with the present limit of $Br(\tau\to\mu\gamma)$.

the present experimental upper limit of $Br(\mathrm{h}\to\mu\tau)$, $Br(\mathrm{h}\to\mu\tau)$ becomes larger and approaches the present experimental limit with increasing δ_{23}^{XX} $(X=L,R)$. Especially in Fig. 3(a), considering nonzero slepton mixing parameters δ_{23}^{LR}, $Br(\mathrm{h}\to\mu\tau)$ can achieve $\mathcal{O}(10^{-4})$, which is below the present experimental limit by just two orders of magnitude. Compared to the MSSM, exotic singlet righthanded neutrino superfields in the μνSSM induce new sources for lepton-flavor violation, considering that the righthanded neutrino and sneutrinos can mix and couple with the other particles seen in Eq. (8) and Appendix A. In Fig. 3(a,c,e), the red triangles overlap with the black circles, because some parameters strongly affect $Br(\tau\to\mu\gamma)$ but do not affect $Br(\mathrm{h}\to\mu\tau)$. We will research this further in the following.

To see how other parameters affect the results, we appropriately fix $\delta_{23}^{LR}=0.02$ and $\delta_{23}^{LL}=\delta_{23}^{RR}=0.2$. Then, we scan the parameter space shown in Table 2, where $\mu=M_2=m_L=m_E\equiv M_{\mathrm{SUSY}}$. In the scanning, we also keep the chargino masses $m_{\chi_\beta}>200$ GeV $(\beta=1,2)$, the neutral fermion masses $m_{\chi_\eta^0}>200$ GeV $(\eta=1,\cdots,7)$, and the scalar masses $m_{S_\alpha,P_\alpha,S_\alpha^\pm}>500$ GeV $(\eta=2,\cdots,8)$, to avoid the range ruled out by the experiments [142]. Then in Fig. 4, we plot $\mathrm{Br}(\mathrm{h}\to\mu\tau)$ respectively versus $\tan\beta$ (a) and M_{SUSY} (b), where the dashed line stands for the upper limit on $\mathrm{Br}(\mathrm{h}\to\mu\tau)$ at 95% CL shown in Eq. (2). We show $\mathrm{Br}(\tau\to\mu\gamma)$ varying with $\tan\beta$ (c) and M_{SUSY} (d) respectively, where the dashed line denotes the present limit of $\mathrm{Br}(\tau\to\mu\gamma)$ which can be seen in Eq. (31). We also picture the muon anomalous magnetic dipole moment Δa_μ versus $\tan\beta$ (e) and M_{SUSY} (f) respectively, where the gray area denotes the Δa_μ at 3.0σ given in Eq. (30). Here, the red triangles are excluded by the present limit of $\mathrm{Br}(\tau\to\mu\gamma)$, the green squares are eliminated by the Δa_μ at 3.0σ, and the black circles conform to both the present limit of $\mathrm{Br}(\tau\to\mu\gamma)$ and the Δa_μ at 3.0σ.

In Fig. 4(d,f), the numerical results show that $Br(\tau\to\mu\gamma)$ and the muon anomalous magnetic dipole moment Δa_μ are decoupling with increasing $M_{\rm SUSY}$. For large $M_{\rm SUSY}$, it is hard to give large contribution to Δa_μ. So, the large $M_{\rm SUSY}$ are easily excluded by the Δa_μ at 3.0σ given in Eq. (30), which can be seen in the graph as the green squares. For small $M_{\rm SUSY}$, there can be a large contribution to $Br(\tau \to \mu\gamma)$. Therefore, the small $M_{\rm SUSY}$ are easily ruled out by the present experimental limit of $Br(\tau \to \mu\gamma)$, shown as the red triangles. In Fig. 4(b), $Br(h \to \mu\tau)$ is non-decoupling with increasing $M_{\rm SUSY}$, which is in agreement with the research in the MSSM [44, 67]. Due to the introduction of slepton mixing parameters, the non-decoupling behaviour of $Br(h\to\mu\tau)$ tends to $\mathcal{O}((m_h/M_{\rm SUSY})^0)$, which is somewhat different from the Appelquist-Carazzone decoupling theorem [150]. (As a side note, in Ref. [151], a non-decoupling behaviour in computation of the Higgs mass showed that it was linked to an ambiguity in the treatment of $\tan\beta$, which is a renormalization scheme dependent parameter.) We can also see that the red triangles overlap with the black circles in Fig. 4(b), because the parameter $\tan\beta$ does not affect $Br(h\to\mu\tau)$ visibly in this parameter space. In Fig. 4(a,c,e), the numerical results show that $Br(h\to\mu\tau)$, $Br(\tau\to\mu\gamma)$ and the muon anomalous magnetic dipole moment Δa_μ can have large values when $\tan\beta$ is large.

Table 1. Scanning parameters for Fig. 3.

parameters	min	max	step
$\tan\beta$	5	50	15
$\mu=M_2$/GeV	500	5000	500
$m_L=m_E$/GeV	500	5000	500
δ^{LR}_{23}	0	0.4	0.02
δ^{LL}_{23}	0	1.0	0.05
δ^{RR}_{23}	0	1.0	0.05

Table 2. Scanning parameters for Fig. 4, where $\mu=M_2=m_L=m_E\equiv M_{\rm SUSY}$.

parameters	min	max	step
$\tan\beta$	5	50	2.5
$M_{\rm SUSY}$/GeV	500	5000	250

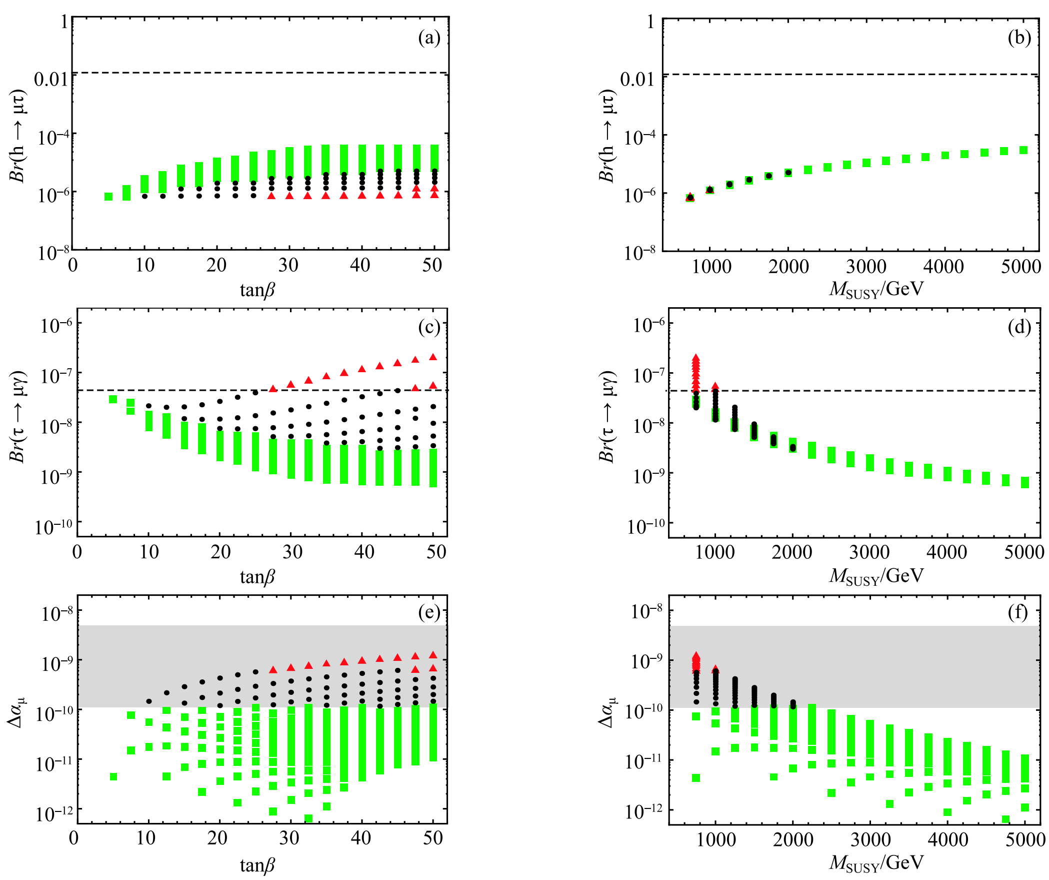

Fig. 4. (color online) $Br(h\to\mu\tau)$ versus $\tan\beta$ (a) and $M_{\rm SUSY}$ (b), where the dashed line stands for the upper limit on $Br(h\to\mu\tau)$ at 95% CL shown in Eq. (2). $Br(\tau\to\mu\gamma)$ versus $\tan\beta$ (c) and $M_{\rm SUSY}$ (d), where the dashed line denotes the present limit of $Br(\tau\to\mu\gamma)$, which can be seen in Eq. (31). Δa_μ versus $\tan\beta$ (e) and $M_{\rm SUSY}$ (f), where the gray area denotes the Δa_μ at 3.0σ given in Eq. (30). Here, the red triangles are excluded by the present limit of $Br(\tau\to\mu\gamma)$, the green squares are eliminated by the Δa_μ at 3.0σ, and the black circles simultaneously conform to the present limit of $Br(\tau\to\mu\gamma)$ and the Δa_μ at 3.0σ.

5 Summary

In this work, we have studied the 125 GeV Higgs decay with lepton flavor violation, $h \to \mu\tau$, in the framework of the $\mu\nu$SSM with slepton flavor mixing. The numerical results show that the branching ratio of $h \to \mu\tau$ depends on the slepton mixing parameters δ_{23}^{XX} $(X = L, R)$, because the lepton flavour violating processes are flavor dependent. The branching ratio of $h \to \mu\tau$ increases with increasing δ_{23}^{XX} $(X = L, R)$. Under the experimental constraints of the muon anomalous magnetic dipole moment, the SM-like Higgs mass around 125 GeV and the present limit of $Br(\tau \to \mu\gamma)$, the branching ratio of $h \to \mu\tau$ can reach $\mathcal{O}(10^{-4})$. Compared with the MSSM, exotic singlet righthanded neutrino superfields in the $\mu\nu$SSM induce new sources for the lepton-flavor violation. Considering that the recent ATLAS and CMS measurements for $h \to \mu\tau$ do not show a significant deviation from the SM, the experiments still need to make more precise measurements in the future. To detect a Higgs boson lepton flavour violating process is a prospective window to search for new physics.

Appendix A

The couplings

The couplings between CP-even neutral scalars and the other CP-even (or CP-odd) neutral scalars are formulated as

$$\mathcal{L}_{\rm int} = C^S_{\alpha\beta\gamma} S_\alpha S_\beta S_\gamma + C^P_{\alpha\beta\gamma} S_\alpha P_\beta P_\gamma, \tag{A1}$$

with

$$\begin{aligned} C^S_{\alpha\beta\gamma} = \frac{-e^2}{4\sqrt{2} s^2_W c^2_W} \Big[& \upsilon_d R_S^{1\alpha} R_S^{1\beta} R_S^{1\gamma} + \upsilon_u R_S^{2\alpha} R_S^{2\beta} R_S^{2\gamma} \\ & + (\upsilon_d R_S^{1\alpha} + \upsilon_u R_S^{2\alpha}) R_S^{(2+i)\beta} R_S^{(2+i)\gamma} \Big] \\ & + \frac{1}{\sqrt{2}} \Big[\lambda_i \lambda_i (\upsilon_d R_S^{1\alpha} R_S^{2\beta} R_S^{2\gamma} + \upsilon_u R_S^{2\alpha} R_S^{1\beta} R_S^{1\gamma}) \\ & - \lambda_i \lambda_j (\upsilon_d R_S^{1\alpha} + \upsilon_u R_S^{2\alpha}) R_S^{(5+i)\beta} R_S^{(5+j)\gamma} \Big] \\ & + \sqrt{2} \kappa_{mij} \kappa_{mkl} \upsilon_{\nu_i^c} R_S^{(5+j)\alpha} R_S^{(5+k)\beta} R_S^{(5+l)\gamma} \\ & - \frac{1}{3\sqrt{2}} (A_\kappa \kappa)_{ijk} R_S^{(5+i)\alpha} R_S^{(5+j)\beta} R_S^{(5+k)\gamma} \\ & + \frac{1}{\sqrt{2}} (A_\lambda \lambda)_i R_S^{1\alpha} R_S^{2\beta} R_S^{(5+i)\gamma} \\ & - \frac{1}{\sqrt{2}} \lambda_i \kappa_{ijk} (\upsilon_u R_S^{1\alpha} + \upsilon_d R_S^{2\alpha}) R_S^{(5+j)\beta} R_S^{(5+k)\gamma}, \end{aligned} \tag{A2}$$

$$\begin{aligned} C^P_{\alpha\beta\gamma} = \frac{-e^2}{4\sqrt{2} s^2_W c^2_W} \Big[& \upsilon_d R_S^{1\alpha} R_P^{1\beta} R_P^{1\gamma} \\ & + \upsilon_u R_S^{2\alpha} R_P^{2\beta} R_P^{2\gamma} + (\upsilon_d R_S^{1\alpha} \\ & + \upsilon_u R_S^{2\alpha}) R_P^{(2+i)\beta} R_P^{(2+i)\gamma} \Big] \\ & + \frac{1}{\sqrt{2}} \Big[\lambda_i \lambda_i (\upsilon_d R_S^{1\alpha} R_P^{2\beta} R_P^{2\gamma} + \upsilon_u R_S^{2\alpha} R_P^{1\beta} R_P^{1\gamma}) \\ & - \lambda_i \lambda_j (\upsilon_d R_S^{1\alpha} + \upsilon_u R_S^{2\alpha}) R_P^{(5+i)\beta} R_P^{(5+j)\gamma} \Big] \\ & + \sqrt{2} \kappa_{mij} \kappa_{mkl} \upsilon_{\nu_i^c} R_S^{(5+l)\alpha} R_P^{(5+j)\beta} R_P^{(5+k)\gamma} \\ & + \frac{1}{\sqrt{2}} (A_\kappa \kappa)_{ijk} R_S^{(5+i)\alpha} R_P^{(5+j)\beta} R_P^{(5+k)\gamma} \\ & - \frac{1}{\sqrt{2}} (A_\lambda \lambda)_i \Big[R_S^{1\alpha} R_P^{2\beta} R_P^{(5+i)\gamma} + R_S^{2\alpha} R_P^{1\beta} R_P^{(5+i)\gamma} \\ & + R_S^{(5+i)\alpha} R_P^{1\beta} R_P^{2\gamma} \Big] \\ & + \frac{1}{\sqrt{2}} \lambda_i \kappa_{ijk} (\upsilon_u R_S^{1\alpha} + \upsilon_d R_S^{2\alpha}) R_P^{(5+j)\beta} R_P^{(5+k)\gamma}, \end{aligned} \tag{A3}$$

where the unitary matrices R_S, R_P (and Z_n, Z_-, Z_+ below) can be found in Ref. [121], and the small terms containing $Y_{\nu_i} \sim \mathcal{O}(10^{-7})$ and $\upsilon_{\nu_i} \sim \mathcal{O}(10^{-4}\,\text{GeV})$ are ignored.

The interaction Lagrangian between CP-even neutral scalars and neutral fermions is formulated as

$$\mathcal{L}_{\rm int} = S_\alpha \bar{\chi}^0_\varsigma \Big(C_L^{S_\alpha \chi^0_\eta \bar{\chi}^0_\varsigma} P_L + C_R^{S_\alpha \chi^0_\eta \bar{\chi}^0_\varsigma} P_R \Big) \chi^0_\eta, \tag{A4}$$

where

$$\begin{aligned} C_L^{S_\alpha \chi^0_\eta \bar{\chi}^0_\varsigma} = & \frac{-e}{2 s_{\rm W} c_{\rm W}} \Big(c_{\rm W} Z_n^{2\eta} - s_{\rm W} Z_n^{1\eta} \Big) \\ & \Big(R_S^{1\alpha} Z_n^{3\varsigma} - R_S^{2\alpha} Z_n^{4\varsigma} + R_S^{(2+i)\alpha} Z_n^{(7+i)\varsigma} \Big) \\ & - \frac{1}{\sqrt{2}} Y_{\nu_{ij}} \Big(R_S^{2\alpha} Z_n^{(7+i)\eta} Z_n^{(4+j)\varsigma} \\ & + R_S^{(2+i)\alpha} Z_n^{3\eta} Z_n^{(4+j)\varsigma} + R_S^{(5+j)\alpha} Z_n^{3\eta} Z_n^{(7+i)\varsigma} \Big) \\ & - \frac{1}{\sqrt{2}} \lambda_i \Big(R_S^{1\alpha} Z_n^{(4+i)\eta} Z_n^{4\varsigma} \\ & + R_S^{2\alpha} Z_n^{(4+i)\eta} Z_n^{3\varsigma} + R_S^{(5+i)\alpha} Z_n^{3\eta} Z_n^{4\varsigma} \Big) \\ & + \frac{1}{\sqrt{2}} \kappa_{ijk} R_S^{(5+i)\alpha} Z_n^{(4+j)\eta} Z_n^{(4+k)\varsigma}, \end{aligned} \tag{A5}$$

$$C_R^{S_\alpha \chi^0_\eta \bar{\chi}^0_\varsigma} = \Big[C_L^{S_\alpha \chi^0_\varsigma \bar{\chi}^0_\eta} \Big]^*, \tag{A6}$$

and

$$P_L = \frac{1}{2}(1-\gamma^5), \qquad P_R = \frac{1}{2}(1+\gamma^5). \tag{A7}$$

The interaction Lagrangian of neutral scalars and charged fermions can be written as

$$\begin{aligned} \mathcal{L}_{\rm int} = & S_\alpha \bar{\chi}_\varsigma (C_L^{S_\alpha \chi_\beta \bar{\chi}_\varsigma} P_L + C_R^{S_\alpha \chi_\beta \bar{\chi}_\varsigma} P_R) \chi_\beta \\ & + P_\alpha \bar{\chi}_\varsigma (C_L^{P_\alpha \chi_\beta \bar{\chi}_\varsigma} P_L + C_R^{P_\alpha \chi_\beta \bar{\chi}_\varsigma} P_R) \chi_\beta, \end{aligned} \tag{A8}$$

where the coefficients are

$$
\begin{aligned}
C_L^{S_\alpha\chi_\beta\bar{\chi}_\zeta} = & \frac{-e}{\sqrt{2}s_{\rm W}}\Big[R_S^{2\alpha}Z_-^{1\beta}Z_+^{2\zeta}+R_S^{1\alpha}Z_-^{2\beta}Z_+^{1\zeta} \\
& +R_S^{(2+i)\alpha}Z_-^{(2+i)\beta}Z_+^{1\zeta}\Big] \\
& -\frac{1}{\sqrt{2}}\lambda_i R_S^{(5+i)\alpha}Z_-^{2\beta}Z_+^{2\zeta} \\
& +\frac{1}{\sqrt{2}}Y_{e_{ij}}\Big[R_S^{(2+i)\alpha}Z_-^{2\beta}Z_+^{(2+j)\zeta} \\
& -R_S^{1\alpha}Z_-^{(2+i)\beta}Z_+^{(2+j)\zeta}\Big] \\
& -\frac{1}{\sqrt{2}}Y_{\nu_{ij}}R_S^{(5+j)\alpha}Z_-^{(2+i)\beta}Z_+^{2\zeta}, \qquad \text{(A9)}
\end{aligned}
$$

$$
\begin{aligned}
C_L^{P_\alpha\chi_\beta\bar{\chi}_\zeta} = & \frac{{\rm i}e}{\sqrt{2}s_{\rm W}}\Big[R_P^{2\alpha}Z_-^{1\beta}Z_+^{2\zeta}+R_P^{1\alpha}Z_-^{2\beta}Z_+^{1\zeta} \\
& +R_P^{(2+i)\alpha}Z_-^{(2+i)\beta}Z_+^{1\zeta}\Big]-\frac{\rm i}{\sqrt{2}}\lambda_i R_P^{(5+i)\alpha}Z_-^{2\beta}Z_+^{2\zeta} \\
& +\frac{\rm i}{\sqrt{2}}Y_{e_{ij}}\Big[R_P^{(2+i)\alpha}Z_-^{2\beta}Z_+^{(2+j)\zeta} \\
& -R_P^{1\alpha}Z_-^{(2+i)\beta}Z_+^{(2+j)\zeta}\Big] \\
& -\frac{\rm i}{\sqrt{2}}Y_{\nu_{ij}}R_P^{(5+j)\alpha}Z_-^{(2+i)\beta}Z_+^{2\zeta}, \qquad \text{(A10)}
\end{aligned}
$$

$$
C_R^{S_\alpha\chi_\beta\bar{\chi}_\zeta}=\Big[C_L^{S_\alpha\chi_\zeta\bar{\chi}_\beta}\Big]^*,\quad C_R^{P_\alpha\chi_\beta\bar{\chi}_\zeta}=\Big[C_L^{P_\alpha\chi_\zeta\bar{\chi}_\beta}\Big]^*. \qquad \text{(A11)}
$$

The interaction Lagrangian of charged scalars, charged fermions, and neutral fermions can be similarly written by

$$
\begin{aligned}
\mathcal{L}_{\rm int} = & S_\alpha^-\bar{\chi}_\beta(C_L^{S_\alpha^-\chi_\eta^0\bar{\chi}_\beta}P_L+C_R^{S_\alpha^-\chi_\eta^0\bar{\chi}_\beta}P_R)\chi_\eta^0 \\
& +S_\alpha^{-*}\bar{\chi}_\eta^0(C_L^{S_\alpha^{-*}\chi_\beta\bar{\chi}_\eta^0}P_L+C_R^{S_\alpha^{-*}\chi_\beta\bar{\chi}_\eta^0}P_R)\chi_\beta, \qquad \text{(A12)}
\end{aligned}
$$

where

$$
\begin{aligned}
C_L^{S_\alpha^-\chi_\eta^0\bar{\chi}_\beta} = & \frac{-e}{\sqrt{2}s_{\rm W}c_{\rm W}}R_{S^\pm}^{2\alpha*}Z_+^{2\beta}\Big[c_{\rm W}Z_n^{2\eta}+s_{\rm W}Z_n^{1\eta}\Big] \\
& -\frac{e}{s_{\rm W}}R_{S^\pm}^{2\alpha*}Z_+^{1\beta}Z_n^{4\eta}-\frac{\sqrt{2}e}{c_{\rm W}}R_{S^\pm}^{(5+i)\alpha*}Z_+^{(2+i)\beta}Z_n^{1\eta} \\
& +Y_{\nu_{ij}}R_{S^\pm}^{(2+i)\alpha}Z_+^{2\beta}Z_n^{(4+j)\eta}+Y_{e_{ij}}Z_+^{(2+j)\beta} \\
& \cdot\Big[R_{S^\pm}^{1\alpha}Z_n^{(7+i)\eta}-R_{S^\pm}^{(2+i)\alpha}Z_n^{3\eta}\Big] \\
& -\lambda_i R_{S^\pm}^{1\alpha}Z_+^{2\beta}Z_n^{(4+i)\eta}, \qquad \text{(A13)}
\end{aligned}
$$

$$
\begin{aligned}
C_L^{S_\alpha^{-*}\chi_\beta\bar{\chi}_\eta^0} = & \frac{e}{\sqrt{2}s_{\rm W}c_{\rm W}}\Big[R_{S^\pm}^{1\alpha*}Z_-^{2\beta}+R_{S^\pm}^{(2+i)\alpha*}Z_-^{(2+i)\beta}\Big] \\
& \cdot\Big[c_{\rm W}Z_n^{2\eta}+s_{\rm W}Z_n^{1\eta}\Big] \\
& -\frac{e}{s_{\rm W}}Z_-^{1\beta}\Big[R_{S^\pm}^{1\alpha*}Z_n^{3\eta}+R_{S^\pm}^{(2+i)\alpha*}Z_n^{(7+i)\eta}\Big] \\
& +Y_{\nu_{ij}}R_{S^\pm}^{2\alpha}Z_-^{(2+i)\beta}Z_n^{(4+j)\eta}+Y_{e_{ij}}R_{S^\pm}^{(5+j)\alpha} \\
& \cdot\Big[Z_-^{2\beta}Z_n^{(7+i)\eta}-Z_-^{(2+i)\beta}Z_n^{3\eta}\Big] \\
& -\lambda_i R_{S^\pm}^{2\alpha}Z_-^{2\beta}Z_n^{(4+i)\eta}, \qquad \text{(A14)}
\end{aligned}
$$

$$
C_R^{S_\alpha^-\chi_\eta^0\bar{\chi}_\beta}=\Big[C_L^{S_\alpha^{-*}\chi_\beta\bar{\chi}_\eta^0}\Big]^*,\quad C_R^{S_\alpha^{-*}\chi_\beta\bar{\chi}_\eta^0}=\Big[C_L^{S_\alpha^-\chi_\eta^0\bar{\chi}_\beta}\Big]^*. \qquad \text{(A15)}
$$

Appendix B

Muon MDM in the μνSSM

The muon anomalous magnetic dipole moment (MDM) in the μνSSM can be given as the effective Lagrangian

$$
\mathcal{L}_{\rm MDM}=\frac{e}{4m_\mu}a_\mu\bar{l}_\mu\sigma^{\alpha\beta}l_\mu F_{\alpha\beta}, \qquad \text{(B1)}
$$

where l_μ denotes the muon which is on-shell, m_μ is the mass of the muon, $\sigma^{\alpha\beta}=\frac{i}{2}[\gamma^\alpha,\gamma^\beta]$, $F_{\alpha\beta}$ represents the electromagnetic field strength and muon MDM $a_\mu=\frac{1}{2}(g-2)_\mu$. Adopting the effective Lagrangian approach, the MDM of the muon can be written by [152–154]

$$
a_\mu=4m_\mu^2\Re(C_2^R+C_2^{L*}+C_6^R), \qquad \text{(B2)}
$$

where $\Re(\cdots)$ denotes the operation to take the real part of the complex number, and $C_{2,6}^{L,R}$ represent the Wilson coefficients of the corresponding effective operators $O_{2,6}^{L,R}$

$$
\begin{aligned}
O_2^{L,R} &= \frac{eQ_f}{(4\pi)^2}\overline{(i\mathcal{D}_\alpha l_\mu)}\gamma^\alpha F\cdot\sigma P_{L,R}l_\mu, \\
O_6^{L,R} &= \frac{eQ_f m_\mu}{(4\pi)^2}\bar{l}_\mu F\cdot\sigma P_{L,R}l_\mu. \qquad \text{(B3)}
\end{aligned}
$$

The SUSY corrections of the Wilson coefficients in the μνSSM can be

$$
C_{2,6}^{L,R}=C_{2,6}^{L,R(n)}+C_{2,6}^{L,R(c)}. \qquad \text{(B4)}
$$

The effective coefficients $C_{2,6}^{L,R(n)}$ denote the contributions from the neutralinos χ_η^0 and the charged scalars S_α^- loops

$$
\begin{aligned}
C_2^{R(n)} = & \frac{1}{m_{\rm W}^2}C_L^{S_\alpha^-\chi_\eta^0\bar{l}_\mu}C_R^{S_\alpha^{-*}l_\mu\bar{\chi}_\eta^0}\Big[-I_3(x_{\chi_\eta^0},x_{S_\alpha^-}) \\
& +I_4(x_{\chi_\eta^0},x_{S_\alpha^-})\Big], \\
C_6^{R(n)} = & \frac{m_{\chi_\eta^0}}{m_{\rm W}^2 m_\mu}C_R^{S_\alpha^-\chi_\eta^0\bar{l}_\mu}C_R^{S_\alpha^{-*}l_\mu\bar{\chi}_\eta^0}\Big[-2I_1(x_{\chi_\eta^0},x_{S_\alpha^-}) \\
& +2I_3(x_{\chi_\eta^0},x_{S_\alpha^-})\Big], \\
C_{2,6}^{L(n)} = & C_{2,6}^{R(n)}\,|_{L\leftrightarrow R}\,. \qquad \text{(B5)}
\end{aligned}
$$

Similarly, the contributions $C_{2,6}^{L,R(c)}$ coming from the charginos χ_β and the neutral scalars N_α $(N=S,P)$ loops are

$$
C_2^{R(c)}=\sum_{N=S,P}\frac{1}{m_{\rm W}^2}C_R^{N_\alpha\chi_\beta\bar{l}_\mu}C_L^{N_\alpha l_\mu\bar{\chi}_\beta}\Big[-I_1(x_{\chi_\beta},x_{N_\alpha})
$$

$$
\begin{aligned}
&+2I_3(x_{\chi_\beta},x_{N_\alpha})-I_4(x_{\chi_\beta},x_{N_\alpha})\Big],\\
C_6^{R(c)}=&\sum_{N=S,P}\frac{m_{\chi_\beta}}{m_{\rm W}^2m_\mu}C_R^{N_\alpha\chi_\beta\bar{l}_\mu}C_R^{N_\alpha l_\mu\bar{\chi}_\beta}\Big[2I_1(x_{\chi_\beta},x_{N_\alpha})\\
&-2I_2(x_{\chi_\beta},x_{N_\alpha})-2I_3(x_{\chi_\beta},x_{N_\alpha})\Big],\\
C_{2,6}^{L(c)}=&C_{2,6}^{R(c)}|_{L\leftrightarrow R}\,.
\end{aligned}
\tag{B6}
$$

Here, the loop functions $I_i(x_1,x_2)$ are given as

$$
I_1(x_1,x_2)=\frac{1}{16\pi^2}\Big[\frac{1+\ln x_2}{x_1-x_2}-\frac{x_1\ln x_1-x_2\ln x_2}{(x_1-x_2)^2}\Big], \tag{B7}
$$

$$
\begin{aligned}
I_2(x_1,x_2)=&\frac{1}{16\pi^2}\Big[-\frac{1+\ln x_1}{x_1-x_2}+\frac{x_1\ln x_1-x_2\ln x_2}{(x_1-x_2)^2}\Big],\\
I_3(x_1,x_2)=&\frac{1}{32\pi^2}\Big[\frac{3+2\ln x_2}{x_1-x_2}+\frac{2x_2+4x_2\ln x_2}{(x_1-x_2)^2}\\
&-\frac{2x_1^2\ln x_1}{(x_1-x_2)^3}+\frac{2x_2^2\ln x_2}{(x_1-x_2)^3}\Big],
\end{aligned}
\tag{B8}
$$

$$
\begin{aligned}
I_4(x_1,x_2)=&\frac{1}{96\pi^2}\Big[\frac{11+6\ln x_2}{x_1-x_2}+\frac{15x_2+18x_2\ln x_2}{(x_1-x_2)^2}\\
&+\frac{6x_2^2+18x_2^2\ln x_2}{(x_1-x_2)^3}-\frac{6x_1^3\ln x_1-6x_2^3\ln x_2}{(x_1-x_2)^4}\Big].
\end{aligned}
\tag{B9}
$$

References

1 G. Aad et al. (ATLAS Collaboration), Phys. Lett. B, **716**: 1 (2012), arXiv:1207.7214 [hep-ex]
2 S. Chatrchyan et al. (CMS Collaboration), Phys. Lett. B, **716**: 30 (2012), arXiv:1207.7235 [hep-ex]
3 G. Aad et al. (ATLAS and CMS Collaborations), Phys. Rev. Lett., **114**: 191803 (2015), arXiv:1503.07589 [hep-ex]
4 R. Harnik, J. Kopp and J. Zupan, JHEP, **03**: 026 (2013), arXiv:1209.1397
5 V. Khachatryan et al. (CMS Collaboration), Phys. Lett. B, **749**: 337–362 (2015), arXiv:1502.07400 [hep-ex]
6 V. Khachatryan et al. (CMS Collaboration), CMS-PAS-HIG-16-005
7 G. Aad et al. (ATLAS Collaboration), JHEP, **11**: 211 (2015), arXiv:1508.03372 [hep-ex]
8 G. Aad et al. (ATLAS Collaboration), arXiv:1604.07730 [hep-ex]
9 J. L. Diaz-Cruz and J. J. Toscano, Phys. Rev. D, **62**: 116005 (2000), arXiv:hep-ph/9910233
10 T. Han and D. Marfatia, Phys. Rev. Lett., **86**: 1442 (2001), arXiv: hep-ph/0008141
11 J.L. Diaz-Cruz, JHEP, **05**: 036 (2003)
12 A. Brignole and A. Rossi, Phys. Lett. B, **566** 217–225 (2003)
13 A. Brignole and A. Rossi, Nucl. Phys. B, **701** 3–53 (2004)
14 E. Arganda, A.M. Curiel, M.J. Herrero and D. Temes, Phys. Rev. D, **71**: 035011 (2005)
15 J. K. Parry, Nucl. Phys. B, **760**: 38–63 (2007)
16 J. L. Diaz-Cruz, D. K. Ghosh and S. Moretti, Phys. Lett. B, **679**: 376–381 (2009)
17 A. Arhrib, Y. Cheng and O. C. W. Kong, Phys. Rev. D, **87**: 015025 (2013), arXiv:1210.8241
18 K. Agashe and R. Contino, Phys. Rev. D, **80**: 075016 (2009), arXiv:0906.1542
19 A. Azatov, M. Toharia and L. Zhu, Phys. Rev. D, **80**: 035016 (2009), arXiv:0906.1990
20 S. Casagrande et al., JHEP, **10**: 094 (2008), arXiv:0807.4937
21 G. Perez and L. Randall, JHEP, **01**: 077 (2009), arXiv:0805.4652
22 A. J. Buras, B. Duling and S. Gori, JHEP, **09**: 076 (2009), arXiv:0905.2318
23 M. Blanke, A. J. Buras, B. Duling et al, JHEP, **03**: 001 (2009), arXiv:0809.1073
24 G. F. Giudice and O. Lebedev, Phys. Lett. B, **665**: 79 (2008), arXiv:0804.1753
25 J. A. Aguilar-Saavedra, Nucl. Phys. B, **821**: 215 (2009), arXiv:0904.2387
26 M. E. Albrecht, M. Blanke, A. J. Buras et al, JHEP, **09**: 064 (2009), arXiv:0903.2415
27 H. Ishimori, T. Kobayashi, H. Ohki et al, Prog. Theor. Phys. Suppl., **183**: 1 (2010), arXiv:1003.3552
28 A. Goudelis, O. Lebedev and J. H. Park, Phys. Lett. B, **707**: 369 (2012), arXiv:1111.1715
29 D. McKeen, M. Pospelov and A. Ritz, Phys. Rev. D, **86**: 113004 (2012), arXiv:1208.4597
30 I. de Medeiros Varzielas, O. Fischer and V. Maurer, JHEP, **08**: 080 (2015), arXiv:1504.03955
31 A. Pilaftsis, Phys. Lett. B, **285**: 68–74 (1992)
32 K. A. Assamagan, A. Deandrea and P.-A. Delsart, Phys. Rev. D, **67**: 035001 (2003), arXiv:hep-ph/0207302
33 S. Kanemura, K. Matsuda, T. Ota et al, Phys. Lett. B, **599**: 83–91 (2004), arXiv:hep-ph/0406316
34 U. Cotti, M. Pineda and G. Tavares-Velasco, arXiv:hep-ph/0501162
35 S. Kanemura, T. Ota and K. Tsumura, Phys. Rev. D, **73**: 016006 (2006) , arXiv:hep-ph/0505191
36 M. Cannoni and O. Panella, Phys. Rev. D, **79**: 056001 (2009), arXiv:0812.2875
37 S. Kanemura and K. Tsumura, Phys. Lett. B, **674**: 295–298 (2009), arXiv:0901.3159
38 S.-L. Chen, M. Frigerio and E. Ma, Phys. Lett. B, **612**: 29–35 (2005), arXiv:hep-ph/0412018
39 M. Cannoni and O. Panella, Phys. Rev. D, **79**: 056001 (2009), arXiv:0812.2875
40 E. Iltan, Mod. Phys. Lett. A, **24**: 1361 (2009), arXiv:0809.3594
41 G. Blankenburg, J. Ellis and G. Isidori, Phys. Lett. B, **712**: 386–390 (2012) , arXiv:1202.5704
42 A. Arhrib, Y. Cheng and O. C. W. Kong, Europhys. Lett., **101**: 31003 (2013), arXiv:1208.4669
43 A. Dery, A. Efrati, Y. Hochberg and Y. Nir, JHEP, **05**: 039 (2013), arXiv:1302.3229
44 M. Arana-Catania, E. Arganda and M. Herrero, JHEP, **09**: 160 (2013) [Erratum-ibid. 10 (2015) 192], arXiv:1304.3371
45 M. Arroyo, J. L. Diaz-Cruz, E. Diaz and J. A. Orduz-Ducuara, arXiv:1306.2343
46 A. Celis, V. Cirigliano and E. Passemar, Phys. Rev. D, **89**: 013008 (2014), arXiv:1309.3564
47 A. Falkowski, D. M. Straub and A. Vicente, JHEP, **05**: 092 (2014), arXiv:1312.5329
48 A. Dery, A. Efrati, Y. Nir et al, Phys. Rev. D, **90**: 115022 (2014), arXiv:1408.1371
49 M. D. Campos, A. E. Carcamo Hernández, H. Päs and E. Schumacher, Phys. Rev. D, **91**: 116011 (2015), arXiv:1408.1652
50 D. Aristizabal Sierra and A. Vicente, Phys. Rev. D, **90**: 115004 (2014), arXiv:1409.7690
51 J. Heeck, M. Holthausen, W. Rodejohann and Y. Shimizu, Nucl. Phys. B, **896**: 281–310 (2015), arXiv:1412.3671
52 A. Crivellin, G. D'Ambrosio and J. Heeck, Phys. Rev. Lett., **114**: 151801 (2015), arXiv:1501.00993
53 I. Dorner, S. Fajfer, A. Greljo, et al, JHEP, **06**: 108 (2015), arXiv:1502.07784
54 Y. Omura, E. Senaha and K. Tobe, JHEP, **05**: 028 (2015),

arXiv:1502.07824
55 A. Crivellin, G. D'Ambrosio and J. Heeck, Phys. Rev. D, **91**: 075006 (2015), arXiv:1503.03477
56 A. Vicente, Adv. High Energy Phys. **2015**: 686572 (2015), arXiv:1503.08622
57 F. Bishara, J. Brod, P. Uttayarat and J. Zupan, JHEP, **01**: 010 (2016), arXiv:1504.04022
58 X.-G. He, J. Tandean and Y.-J. Zheng, JHEP, **09**: 093 (2015), arXiv:1507.02673
59 W. Altmannshofer, S. Gori, A. L. Kagan et al, Phys. Rev. D, **93**: 031301 (2016), arXiv:1507.07927
60 K. Cheung, W.-Y. Keung and P.-Y. Tseng, Phys. Rev. D, **93**: 015010 (2016), arXiv:1508.01897
61 E. Arganda, M. J. Herrero, X. Marcano and C. Weiland, Phys. Rev. D, **93**: 055010 (2016), arXiv:1508.04623
62 F. J. Botella, G. C. Branco, M. Nebot and M. N. Rebelo, Eur. Phys. J. C, **76**: 161 (2016), arXiv:1508.05101
63 X. Liu, L. Bian, X.-Q. Li and J. Shu, Nucl. Phys. B, **909**: 507-524 (2016), arXiv:1508.05716
64 S. Baek and K. Nishiwaki, Phys. Rev. D, **93**: 015002 (2016), arXiv:1509.07410
65 W. Huang and Y.-L. Tang, Phys. Rev. D, **92**: 094015 (2015), arXiv:1509.08599
66 S. Baek and Z. Kang, JHEP, **03**: 106 (2016), arXiv:1510.00100
67 E. Arganda, M.J. Herrero, R. Morales and A. Szynkman, JHEP, **03**: 055 (2016), arXiv:1510.04685
68 D. Aloni, Y. Niry and E. Stamouz, JHEP, **1604**: 162 (2016), arXiv:1511.00979
69 P. T. Giang, L.T. Hue, D.T. Huong and H. N. Long, Nucl. Phys. B, **864**: 85–112 (2012), arXiv:1204.2902
70 D. T. Binh, L. T. Hue, D. T. Huong and H. N. Long, Eur. Phys. J. C, **74**: 2851 (2014), arXiv:1308.3085
71 R. Harnik, J. Kopp and J. Zupan, JHEP, **03**: 026 (2013), arXiv:1209.1397
72 S. Davidson and P. Verdier, Phys. Rev. D, **86**: 111701 (2012), arXiv:1211.1248
73 E. Arganda, M. J. Herrero, X. Marcano and C. Weiland, Phys. Rev. D, **91**: 015001 (2015), arXiv:1405.4300
74 S. Bressler, A. Dery and A. Efrati, Phys. Rev. D, **90**: 015025 (2014), arXiv:1405.4545
75 J. Kopp and M. Nardecchia, JHEP, **10**: 156 (2014), arXiv:1406.5303
76 M. A. López-Osorio, E. Martínez-Pascual and J. J. Toscano, J. Phys. G: Nucl. Part. Phys., **43**: 025003 (2016), arXiv:1408.3307
77 C.-J. Lee and J. Tandean, JHEP, **04**: 174 (2015), arXiv:1410.6803
78 L. de Lima, C. S. Machado, R. D. Matheus and L. A. F. do Prado, JHEP, **11**: 074 (2015), arXiv:1501.06923
79 I. M. Varzielas and G. Hiller, arXiv:1503.01084
80 D. Das and A. Kundu, Phys. Rev. D, **92**: 015009 (2015), arXiv:1504.01125
81 B. Bhattacherjee, S. Chakraborty and S. Mukherjee, Mod. Phys. Lett. A, **31**: 1650174 (2016), arXiv:1505.02688
82 Y. Mao and S. Zhu, Phys. Rev. D, **93**: 035014 (2016), arXiv:1505.07668
83 R. Benbrik, C.-H. Chen and T. Nomura, Phys. Rev. D, **93**: 095004 (2016), arXiv:1511.08544
84 Y. Omura, E. Senaha and K. Tobe, Phys. Rev. D, **94**: 055019 (2016), arXiv:1511.08880
85 M. Sher and K. Thrasher, Phys. Rev. D, **93**: 055021 (2016), arXiv:1601.03973
86 M. Buschmann, J. Kopp, J. Liu and X.-P. Wang, JHEP, **1606**: 149 (2016), arXiv:1601.02616
87 Y. Farzan and I. M. Shoemaker, JHEP, **07**: 033 (2016), arXiv:1512.09147
88 N. Bizot, S. Davidson, M. Frigerio, and J.-L. Kneur, JHEP, **03**: 073 (2016), arXiv:1512.08508
89 C.-F. Chang, C.-H. V. Chang, C. S. Nugroho, and T.-C. Yuan, Nucl. Phys. B, **910**: 293–308 (2016), arXiv:1602.00680
90 C.-H. Chen and T. Nomura, Eur. Phys. J. C, **76**: 353 (2016), arXiv:1602.07519
91 C. Alvarado, R.M. Capdevilla, A. Delgado and A. Martin, arXiv:1602.08506
92 A. Hayreter, X.-G. He and G. Valencia, Phys. Lett. B, **760**: 175–177 (2016), arXiv:1603.06326
93 K. Huitu, V. Keus, N. Koivunen and O. Lebedev, JHEP, **1605**: 026 (2016), arXiv:1603.06614
94 T. T. Thuc, L. T. Hue, H. N. Long and T. P. Nguyen, Phys. Rev. D, **93**: 115026 (2016), arXiv:1604.03285
95 S. Baek, T. Nomura and H. Okada, Phys. Lett. B, **759**: 91–98 (2016), arXiv:1604.03738
96 J. Herrero-Garcia, N. Rius and A. Santamaria, arXiv:1605.06091
97 K. H. Phan, H. T. Hung and L. T. Hue, arXiv:1605.07164
98 S. V. Demidov and I.V. Sobolev, JHEP, **1608**: 030 (2016), arXiv:1605.08220
99 B. Yang, J. Han and N. Liu, arXiv:1605.09248
100 A. Hayreter, X.-G. He and G. Valencia, Phys. Rev. D, **94**: 075002 (2016), arXiv:1606.00951
101 L. Wang, S. Yang and X.-F. Han, arXiv:1606.04408
102 A. Efrati, J. F. Kamenik and Y. Nir, arXiv:1606.07082
103 A. D. Iura, J. Herrero-Garcia and D. Meloni, Nucl. Phys. B, **911**: 388–424 (2016), arXiv:1606.08785
104 M. Aoki, S. Kanemura, K. Sakurai and H. Sugiyama, arXiv:1607.08548
105 S. Fathy, T. Ibrahim, A. Itani and P. Nath, arXiv:1608.05998
106 D. E. López-Fogliani and C. Muñoz, Phys. Rev. Lett., **97**: 041801 (2006), hep-ph/0508297
107 N. Escudero, D.E. López-Fogliani, C. Muñoz and R. Ruiz de Austri, JHEP, **12**: 099 (2008) arXiv:0810.1507
108 J. Fidalgo, D. E. López-Fogliani, C. Muñoz and R. Ruiz de Austri, JHEP, **10**: 020 (2011), arXiv:1107.4614
109 H. P. Nilles, Phys. Rept., **110**: 1 (1984)
110 H. E. Haber and G.L. Kane, Phys. Rept., **117**: 75 (1985)
111 H. E. Haber, hep-ph/9306207
112 S. P. Martin, hep-ph/9709356
113 J. Rosiek, Phys. Rev. D, **41**: 3464 (1990), hep-ph/9511250
114 J. E. Kim and H. P. Nilles, Phys. Lett. B, **138**: 150 (1984)
115 P. Ghosh and S. Roy, JHEP, **04**: 069 (2009), arXiv:0812.0084
116 A. Bartl, M. Hirsch, S. Liebler et al. JHEP, **05**: 120 (2009), arXiv:0903.3596
117 J. Fidalgo, D. E. López-Fogliani, C. Muñoz and R.R. de Austri, JHEP, **08**: 105 (2009), arXiv:0904.3112
118 P. Ghosh, P. Dey, B. Mukhopadhyaya and S. Roy, JHEP, **05**: 087 (2010), arXiv:1002.2705
119 H.-B. Zhang, T.-F. Feng, L.-N. Kou and S.-M. Zhao, Int. J. Mod. Phys. A, **28**: 1350117 (2013), arXiv:1307.6284
120 H.-B. Zhang, T.-F. Feng, S.-M. Zhao and T.-J. Gao, Nucl. Phys. B, **873**: 300 (2013), arXiv:1304.6248
121 H.-B. Zhang, T.-F. Feng, G.-F. Luo et al, JHEP, **07**: 069 (2013) [Erratum-ibid. **10**: 173 (2013)], arXiv:1305.4352
122 H.-B. Zhang, T.-F. Feng, S.-M. Zhao and F. Sun, Int. J. Mod. Phys. A, **29**: 1450123 (2014), arXiv:1407.7365
123 H.-B. Zhang, T.-F. Feng, F. Sun et al, Phys. Rev. D, **89**: 115007 (2014), arXiv:1307.3607
124 G. 't Hooft and M. Veltman, Nucl. Phys. B, **153**: 365 (1979)
125 R. Mertig, M. Bohm and A. Denner, Comput. Phys. Commun., **64**: 345 (1991)
126 A. Denner, Fortsch. Phys., **41**: 307 (1993)
127 A. Denner and S. Dittmaier, Nucl. Phys. B, **658**: 175–202 (2003)
128 T. Hahn and M. Perez-Victoria, Comput. Phys. Commun., **118**: 153 (1999)
129 T. Hahn, Comput. Phys. Commun., **140**: 418 (2001)
130 T. Hahn and C. Schappacher, Comput. Phys. Commun., **143**: 54 (2002)

131 S. Heinemeyer et al. (LHC Higgs Cross Section Working Group), CERN-2013-004, arXiv:1307.1347 [hep-ph]

132 M. Misiak, S. Pokorski and J. Rosiek, Adv. Ser. Direct. High Energy Phys., **15**: 795 (1998), hep-ph/9703442

133 P. Paradisi, JHEP, **10** : 006 (2005), hep-ph/0505046

134 J. Girrbach, S. Mertens, U. Nierste and S. Wiesenfeldt, JHEP, **05**: 026 (2010), arXiv:0910.2663

135 J. Rosiek, P. H. Chankowski, A. Dedes et al, Comput. Phys. Commun., **181**: 2180 (2010), arXiv:1003.4260

136 M. Arana-Catania, S. Heinemeyer and M. J. Herrero, Phys. Rev. D, **88**: 015026 (2013), arXiv:1304.2783

137 H.-B. Zhang, T.-F. Feng, Z.-F. Ge and S.-M. Zhao, JHEP, **02**: 012 (2014), arXiv:1401.2704

138 H.-B. Zhang, G.-L. Luo, T.-F. Feng et al, Mod. Phys. Lett. A, **29**: 1450196 (2014), arXiv:1409.6837

139 M. Carena, J. R. Espinosa, M. Quirós and C. E. M. Wagner, Phys. Lett. B, **355**: 209 (1995)

140 M. Carena, M. Quirós and C. E. M. Wagner, Nucl. Phys. B, **461**: 407 (1996)

141 M. Carena, S. Gori, N.R. Shah and C. E. M. Wagner, JHEP, **03**: 014 (2012)

142 K. A. Olive et al. (Particle Data Group), Chin. Phys. C, **38**: 090001 (2014)

143 G. W. Bennett et al. (Muon (g-2) Collaboration), Phys. Rev. D, **73**: 072003 (2006)

144 P. J. Mohr, B. N. Taylor and D.B. Newell, Rev. Mod. Phys. **80**: 633 (2008)

145 ATLAS Collaboration, Phys. Rev. D, **86**: 092002 (2012)

146 ATLAS Collaboration, JHEP, **10**: 130 (2013)

147 CMS Collaboration, JHEP, **01**: 077 (2013)

148 CMS Collaboration, JHEP, **07**: 122 (2013)

149 B. Aubert et al. (BaBar Collaboration), Phys. Rev. Lett., **104**: 021802 (2010), arXiv:0908.2381

150 T. Appelquist and J. Carazzone, Phys. Rev. D, **11**: 2856 (1975)

151 P. Draper and H. E. Haber, Eur. Phys. J. C, **73**: 2522 (2013)

152 T. F. Feng, L. Sun and X. Y. Yang, Nucl. Phys. B, **800**: 221 (2008)

153 T. F. Feng, L. Sun and X. Y. Yang, Phys. Rev. D, **77**: 116008 (2008)

154 T. F. Feng and X. Y. Yang, Nucl. Phys. B, **814**: 101 (2009)